International Journal of Modern Physics E
Vol. 17, No. 8 (2008) 1441–1452


World Scientific
www.worldscientific.com

# PAIRING PROPERTIES OF SYMMETRIC NUCLEAR MATTER IN RELATIVISTIC MEAN FIELD THEORY

J. LI[*,†] B. Y. SUN[*] and J. MENG[*,‡,§,¶,‖]

[*] *School of Phyics, and State Key Laboratory of Nuclear Physics and Technology, Peking University, Beijing, 100871, China*
[†] *Dipartimento di Fisica, Università degli Studi and INFN Sez. di Milano, Milano, 20133, Italy*
[‡] *Institute of Theoretical Physics, Chinese Academy of Sciences, Beijing, 100080, China*
[§] *Center of Theoretical Nuclear Physics, National Laboratory of Heavy Ion Accelerator, Lanzhou, 730000, China*
[¶] *Department of Physics, University of Stellenbosch, Stellenbosch, South Africa*
[‖] *mengj@pku.edu.cn*

Received 4 June 2008

The properties of pairing correlations in symmetric nuclear matter are studied in the relativistic mean field (RMF) theory with the effective interaction, PK1. Considering the well-known problem that the pairing gap at the Fermi surface calculated with RMF effective interactions is three times larger than that with the Gogny force, an effective factor in the particle–particle channel is introduced. For the RMF calculation with PK1, an effective factor of 0.76 gives a maximum pairing gap of 3.2 MeV at a Fermi momentum of 0.9 $\mathrm{fm}^{-1}$, which is consistent with the result with the Gogny force.

*Keywords*: Pairing correction; relativistic Hartree–Bogoliubov theory; symmetric nuclear matter; effective pairing interaction.

## 1. Introduction

For several years, mean field theory, including non-relativistic mean field theory with effective nucleon–nucleon interactions such as Skyrme or Gogny, and relativistic mean field (RMF) theory, has received a great deal of attention due to its successful descriptions of many nuclear phenomena. In the framework of the RMF theory,[1] nucleons interact via the exchanges of mesons and photons. Representations with large scalar and vector fields in nuclei provide simpler and more efficient descriptions than non-relativistic approaches, which neglect these scales. In this sense, RMF theory is more fundamental. With a limited number of free parameters, i.e. meson masses and meson–nucleon coupling constants, RMF theory has proved to be successful at quantitatively describing the properties of nuclear

matter and neutron stars,[2] nuclei near the valley of stability,[3–5] and exotic nuclei with large neutron or proton excess with the proper treatment of the pairing correlations and continuum effects.[6–9] The theory naturally provides the spin-orbit potential, the origin of the pseudo-spin symmetry[10,11] as a relativistic symmetry,[12–15] and the spin symmetry in the anti-nucleon spectrum.[16]

Since the 1950s, a large number of striking experimental facts, such as the binding energy difference between even–even and odd–even nuclei and a systematic reduction of the moments of inertia of even–even nuclei compared with their neighboring odd–even nuclei in deformed nuclei, suggest the existence of superfluid phenomena in such systems.[17] In astrophysics, the origin of pulsar glitches,[18] namely, sudden discontinuities in the spin-down of pulsars, can also be understood via superfluidity in the inner crust of these stars. All of these phenomena suggest that pairing correlations play an important role in the theoretical study of the properties of nuclei structure and nuclear matter.

The first relativistic study of superfluidity in infinite nuclear matter was done by Kucharek and Ring in 1991.[19] They studied the pairing correlations in symmetric nuclear matter using the relativistic Hartree–Bogoliubov (RHB) method with a one-boson-exchange (OBE) potential in the particle–particle channel. However, the resulting pairing gap at the Fermi surface was found to be about three times larger than that with the Gogny force.[20] Therefore, the effective pairing interaction used in the RHB calculation is either the finite range Gogny force or the Skyrme type zero-range force. In particular, with the Skyrme type zero-range force, various achievements have been made to describe nuclei far from the line of $\beta$-stability with the proper treatment of the pairing correlations and continuum effects.[6–9]

However, it is still an open problem as to how the same nucleon interaction via the exchanges of mesons and photons in the Hartree channel can also be used in the particle–particle channel. In fact, the large pairing gap in the RHB calculation with an OBE potential in the particle–particle channel comes from the behavior of the pairing matrix elements at large momenta.[21] The various effective forces in RMF models are adjusted for mean-field calculations in the Hartree channel only, i.e. only for momenta below the Fermi momentum, thus a realistic particle–particle interactions can have very different behaviors at high momenta. Therefore, in order to get reasonable values for the pairing gap, one can use a suitable value of cut-off in the momentum space in the relativistic mean field calculations,[5,21–23] or consider various effects, such as the medium polarization, the in-medium meson mass decrease, and the mesons' nonlinear terms to reduce the pairing gap in nuclear matter.[24–26]

In this paper, the properties of pairing correlations in symmetric nuclear matter are studied in the RMF theory with the newly developed effective interaction, PK1.[27] In order to solve the well-known problem that the pairing gap at the Fermi surface calculated with RMF effective interactions is three times larger than that with the Gogny force, an effective factor in the particle–particle channel will be introduced. In Sec. 2, a brief description of the RMF theory and RHB theory for

nuclear matter is presented. The results and a discussion are given in Sec. 3. Finally, in the last section, a brief summary is given.

## 2. Theoretical Framework

### 2.1. *Relativistic mean field theory*

A general review of RMF theory and its application in nuclear physics can be found in Refs. 3–5. Here, a brief review of RMF theory for nuclear matter is given. The starting point of RMF theory is an effective Lagrangian density with nucleons interacting via the exchange of various mesons and photons:

$$\begin{aligned}\mathcal{L} = \bar{\psi}\left[i\gamma^\mu\partial_\mu - m - g_\sigma\sigma - g_\omega\gamma^\mu\omega_\mu - g_\rho\gamma^\mu\vec{\tau}\cdot\vec{\rho}_\mu - e\gamma^\mu\frac{1-\tau_3}{2}A_\mu\right]\psi \\ + \frac{1}{2}\partial^\mu\sigma\partial_\mu\sigma - \frac{1}{2}m_\sigma^2\sigma^2 - U(\sigma) - \frac{1}{4}\Omega^{\mu\nu}\Omega_{\mu\nu} + \frac{1}{2}m_\omega^2\omega^\mu\omega_\mu + U(\omega) \\ - \frac{1}{4}\vec{R}^{\mu\nu}\vec{R}_{\mu\nu} + \frac{1}{2}m_\rho^2\vec{\rho}^{\,\mu}\cdot\vec{\rho}_\mu - \frac{1}{4}A^{\mu\nu}A_{\mu\nu}\,. \end{aligned} \tag{1}$$

The Dirac spinor $\psi$ denotes the nucleon with mass $m$. The isoscalar scalar $\sigma$-meson and isoscalar vector $\omega$-meson offer medium-range attractive and short-range repulsive interactions, respectively, and the isovector vector $\rho$-meson provides the necessary isospin asymmetry. Their masses are denoted by $m_\sigma$, $m_\omega$ and $m_\rho$. $g_\sigma$, $g_\omega$ and $g_\rho$ correspond to the meson–nucleon coupling constants. $\tau$ is the isospin of the nucleon, and $\tau_3$ is its three-component. The nonlinear $\sigma$ and $\omega$ self-interactions, $U(\sigma)$ and $U(\omega)$, are respectively denoted as

$$U(\sigma) = \frac{1}{3}g_2\sigma^3 + \frac{1}{4}g_3\sigma^4, \quad U(\omega) = \frac{1}{4}c_3(\omega^\mu\omega_\mu)^2\,, \tag{2}$$

with the self-coupling constants $g_2$, $g_3$ and $c_3$. The field tensors $\Omega_{\mu\nu}$, $\vec{R}_{\mu\nu}$ and $A_{\mu\nu}$ are

$$\Omega_{\mu\nu} = \partial_\mu\omega_\nu - \partial_\nu\omega_\mu, \quad \vec{R}_{\mu\nu} = \partial_\mu\vec{\rho}_\nu - \partial_\nu\vec{\rho}_\mu, \quad A_{\mu\nu} = \partial_\mu A_\nu - \partial_\nu A_\mu\,. \tag{3}$$

The classical variation principle gives the following equations of motion:

$$\left[i\gamma^\mu\partial_\mu - m - g_\sigma\sigma - g_\omega\gamma^\mu\omega_\mu - g_\rho\gamma^\mu\vec{\tau}\cdot\vec{\rho}_\mu - e\gamma^\mu\frac{1-\tau_3}{2}A_\mu\right]\psi = 0\,, \tag{4}$$

for the nucleon spinors, and

$$(\partial^\mu\partial_\mu + m_\sigma^2)\sigma = -g_\sigma\bar{\psi}\psi - g_2\sigma^2 - g_3\sigma^3\,, \tag{5}$$

$$\partial_\mu\Omega^{\mu\nu} + m_\omega^2\omega^\nu = g_\omega\bar{\psi}\gamma^\nu\psi - c_3(\eta^\nu\omega^\nu)^3\,, \tag{6}$$

$$\partial_\mu\vec{R}^{\mu\nu} + m_\rho^2\vec{\rho}^{\,\nu} = g_\rho\bar{\psi}\gamma^\nu\vec{\tau}\psi + g_\rho\vec{\rho}_\mu\times\vec{R}^{\mu\nu}\,, \tag{7}$$

$$\partial_\mu A^{\mu\nu} = e\bar{\psi}\gamma^\nu\frac{1-\tau_3}{2}\psi\,, \tag{8}$$

for the mesons and photons, where the sum over all the particle states in the no-sea approximation is adopted for the source term in Eqs. (5)–(8).

### 2.2. *Relativistic Hartree–Bogoliubov theory*

Usually, in RMF theory, mesons are treated as classical fields. In order to describe the superfluidity of the nuclear many-body system, one needs to quantize not only the nucleon but also the meson fields. By using the well-known canonical quantization method and Green's function techniques, neglecting retardation effects and the Fock term as is mostly done in RMF, one gets the so-called relativistic Hartree–Bogoliubov (RHB) equation[19]:

$$\begin{pmatrix} h-\lambda & \Delta \\ -\Delta^* & -h^*+\lambda \end{pmatrix} \begin{pmatrix} U_k \\ V_k \end{pmatrix} = e_k \begin{pmatrix} U_k \\ V_k \end{pmatrix}, \tag{9}$$

where

$$h = \boldsymbol{\alpha}\cdot\boldsymbol{p} + V + \beta(M+S) \tag{10}$$

is the Dirac Hamiltonian with the scalar potential $S$ and vector potential $V$:

$$S = g_\sigma\sigma, \quad V = \beta\left(g_\omega\gamma^\mu\omega_\mu + g_\rho\gamma^\mu\vec{\tau}\cdot\vec{\rho}_\mu + e\gamma^\mu\frac{1-\tau_3}{2}A_\mu\right). \tag{11}$$

The pairing field is

$$\Delta_{ab} = \frac{1}{2}\sum_{cd}\bar{V}_{abcd}\kappa_{cd}, \tag{12}$$

where $\bar{V}_{abcd}$ is the two-body effective interaction in the particle–particle ($pp$) channel and the pairing tensor $\kappa_{ab} = \sum_k V^*_{ak}U_{bk}$. The quasi-particle eigenvectors are denoted as $(U_k, V_k)$, and $e_k$ represents its corresponding quasi-particle energies.

The chemical potential $\lambda$ in Eq. (9) is determined by the particle number with the subsidiary condition, $\sum_k V_k^2 = N$.

### 2.3. *Application to symmetric nuclear matter*

For static, uniform infinite nuclear matter, the coulomb field is neglected, and the space-like components as well as the differential of the time-like components of the meson fields vanish. Furthermore, for symmetric nuclear matter, the $\rho$-meson has no contribution to the mean field potential. Then, the scalar potential $S$ and vector potential $V$ are constants and have the simple form

$$S = g_\sigma\langle\sigma\rangle, \qquad V = g_\omega\langle\omega_0\rangle\,. \tag{13}$$

The RHB equation (9) can be decomposed into $(2\times 2)$ matrices of BCS-type[19]:

$$\begin{pmatrix} \varepsilon(k)-\lambda & \Delta(k) \\ \Delta(k) & -\varepsilon(k)+\lambda \end{pmatrix} \begin{pmatrix} u(k) \\ v(k) \end{pmatrix} = e(k) \begin{pmatrix} u(k) \\ v(k) \end{pmatrix}, \tag{14}$$

where the eigenvalue of the Dirac Hamiltonian for positive energies is denoted as $\varepsilon(k) = V + \sqrt{k^2 + (m+S)^2}$, the Fermi energy $\lambda = \varepsilon(k_{\rm F})$, and the quasi-particle energy $e(k) = \sqrt{(\varepsilon(k) - \lambda)^2 + \Delta^2(k)}$. The corresponding occupation numbers $v^2(k)$ have the form

$$v^2(k) = \frac{1}{2}\left(1 - \frac{\varepsilon(k) - \lambda}{\sqrt{[\varepsilon(k) - \lambda]^2 + \Delta(k)^2}}\right). \tag{15}$$

The pairing field $\Delta(k)$ obeys the usual gap equation:

$$\Delta(k) = -\frac{1}{8\pi^2}\int_0^\infty f \cdot v_{pp}(k,p)\frac{\Delta(p)}{\sqrt{(\varepsilon(p) - \lambda)^2 + \Delta^2(p)}}p^2 dp\,, \tag{16}$$

where $f$ is an effective factor introduced to reduce the pairing potential. The effective interaction in the $pp$ channel $v_{pp}(k,p)$ is the one-meson exchange potential:

$$v_{pp}(k,p) = v_{pp}^{\sigma}(k,p) + v_{pp}^{\omega}(k,p) + v_{pp}^{\rho}(k,p), \tag{17}$$

where

$$v_{pp}^{\sigma}(p,k) = \frac{g_\sigma^2}{2\varepsilon^*(k)\varepsilon^*(p)}\left\{\frac{(\varepsilon^*(p) - \varepsilon^*(k))^2 + m_\sigma^2 - 4m^{*2}}{4pk}\ln\frac{(k+p)^2 + m_\sigma^2}{(k-p)^2 + m_\sigma^2} - 1\right\}, \tag{18}$$

$$v_{pp}^{\omega}(p,k) = \frac{g_\omega^2}{\varepsilon^*(k)\varepsilon^*(p)}\frac{2\varepsilon^*(k)\varepsilon^*(p) - m^{*2}}{2pk}\ln\frac{(k+p)^2 + m_\omega^2}{(k-p)^2 + m_\omega^2}\,, \tag{19}$$

$$v_{pp}^{\rho}(p,k) = \frac{g_\rho^2}{\varepsilon^*(k)\varepsilon^*(p)}\frac{2\varepsilon^*(k)\varepsilon^*(p) - m^{*2}}{2pk}\ln\frac{(k+p)^2 + m_\rho^2}{(k-p)^2 + m_\rho^2}\,, \tag{20}$$

with effective mass $m^* = m + g_\sigma\sigma$, and $\varepsilon^*(k) = \sqrt{k^2 + m^{*2}}$.

The meson fields are replaced by their mean values and can be solved from the corresponding equations of motion by the various given nucleon densities:

$$m_\sigma^2\sigma = -g_\sigma\rho_s - g_2\sigma^2 - g_3\sigma^3\,, \tag{21}$$

$$m_\omega^2\omega_0 = g_\omega\rho_v - c_3\omega_0^3\,, \tag{22}$$

where $\rho_s$ and $\rho_v$ are, respectively, the scalar- and baryon-density:

$$\rho_s = \bar{\psi}\psi = \frac{2}{\pi^2}\int_0^\infty \frac{m + g_\sigma\sigma}{\sqrt{k^2 + (m + g_\sigma\sigma)^2}}v^2(k)k^2 dk\,, \tag{23}$$

$$\rho_v = \psi^\dagger\psi = \frac{2}{\pi^2}\int_0^\infty v^2(k)k^2 dk\,. \tag{24}$$

## 3. Results and Discussion

For a given Fermi momentum $k_{\rm F}$, the coupled equations (14), (16), (21) and (22) can be solved self-consistently by iteration. The properties of $^1S_0$ pairing correlations of symmetric nuclear matter are studied with the newly developed effective interaction, PK1, which takes into account the self-interactions of the $\sigma$-meson and $\omega$-meson as well as the isospin dependence of the nuclear matter.[27]

The momentum integration in the gap equation, in principle, should go to infinity. In actual calculations, it is necessary to have a cut-off in the momentum space and the convergence of the pairing gap on the cut-off momentum should be checked. The dependence of the pairing gap on the cut-off momentum for different Fermi momenta is given in Fig. 1. The results indicate that the cut-off momentum $k_{\rm C} \geq 10$ fm$^{-1}$ will guarantee the numerical convergence. In the following, $k_{\rm C} = 20$ fm$^{-1}$ will be adopted and the corresponding effective interaction in the $pp$ channel, the momentum-dependence of the pairing gap, and the influence of effective interactions on the pairing gap at the Fermi surface, etc., will be investigated.

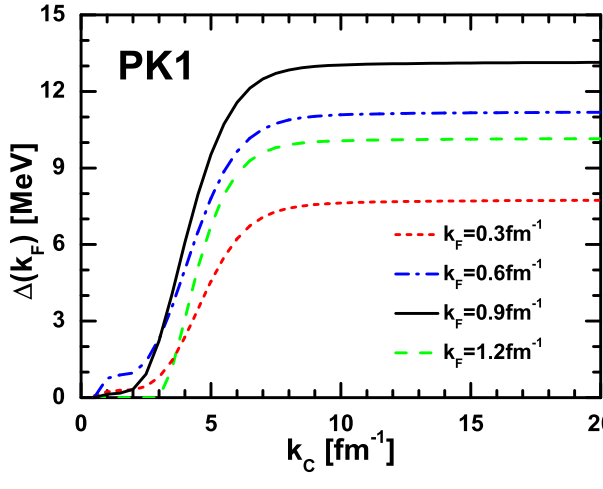


Fig. 1. (Color online) The pairing gap $\Delta(k_{\rm F})$ at the Fermi surface as a function of the cut-off momentum $k_{\rm C}$ in momentum space for different Fermi momenta $k_{\rm F} = 0.3$, 0.6, 0.9 and 1.2 fm$^{-1}$ with the effective interaction, PK1.

### 3.1. *The effective interaction in the pp channel*

The contour plot for the effective interaction in the $pp$ channel $v_{pp}(k, p)$ for different Fermi momenta with the effective interaction PK1 is shown in Fig. 2, where the contours with negative values are denoted by dashed lines.

The interaction is attractive for small and repulsive for larger momenta $k$ and $p$, or equivalently, attractive for large distances and repulsive for small distances.

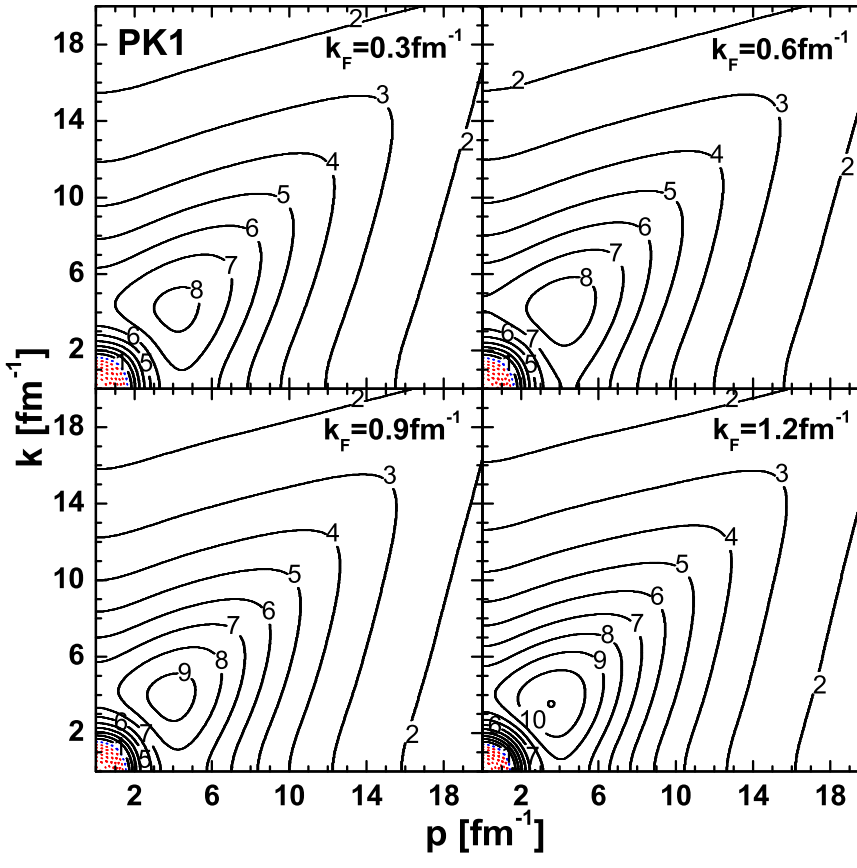


Fig. 2. (Color online) Contour plots for the effective interaction in the $pp$ channel $v_{pp}(k,p)$ as a function of the momenta $p$ and $k$ for different Fermi momenta $k_{\rm F} = 0.3$, 0.6, 0.9 and 1.2 fm$^{-1}$ with the effective interaction, PK1. The contour lines have a distance of 1 (fm$^2$) and the negative values are denoted by dashed lines.

At around 1.5 fm$^{-1}$, the interaction will change from being attractive to being repulsive. The repulsive interaction reaches its maximum value at the momenta $k$ and $p$ around 4 fm$^{-1}$. The maximum repulsive interaction increases with the Fermi momentum.

The behavior of the effective interaction in the $pp$ channel $v_{pp}(k,p)$ can be understood from the contributions of different mesons, as shown in Fig. 3. The scalar meson $\sigma$ provides the attractive part of the effective interaction, $v^{\sigma}_{pp}(p,k)$, with a peak value at zero momentum, and approaching zero with increasing momentum. While the vector mesons $\omega$ and $\rho$ provide the repulsive part, extending to higher momenta than $v^{\sigma}_{pp}(p,k)$. The main contribution for the repulsive part comes from the $\omega$-meson, as seen in the figures; $v^{\omega}_{pp}(p,k)$ is one order of magnitude larger than $v^{\rho}_{pp}(p,k)$.

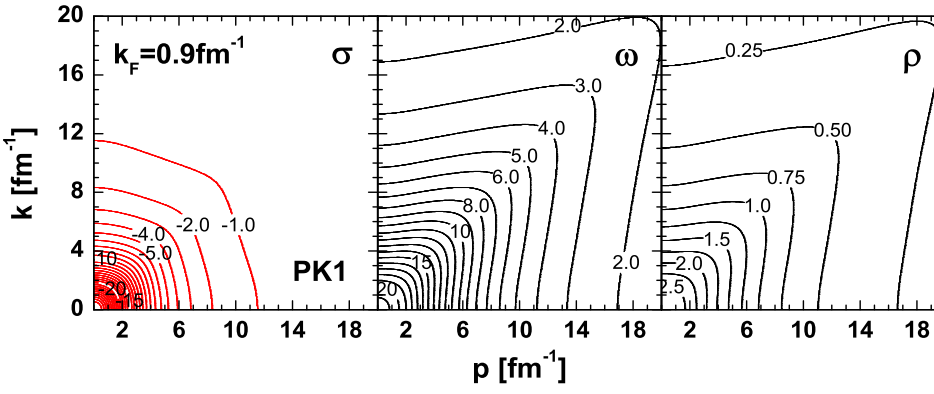


Fig. 3. (Color online) Contour lines of different meson contributions for the effective interaction in the $pp$ channel $v_{pp}(k,p)$ as a function of the momenta $p$ for Fermi momentum $k_{\rm F} = 0.9$ fm$^{-1}$ with the effective interaction, PK1. The contour lines have units of fm$^2$ and the negative contours are shown in red.

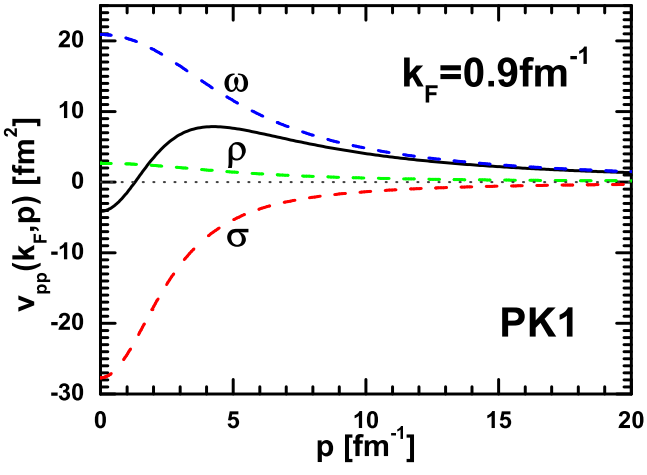


Fig. 4. (Color online) Different meson contributions to the effective interaction in the $pp$ channel $v_{pp}(k,p)$ as a function of $p$ at $k = k_{\rm F} = 0.9$ fm$^{-1}$ with the effective interaction, PK1. The dashed lines corresponds to the contributions from the $\sigma$-, $\omega$- and $\rho$-fields; the solid line represents the total contribution.

Different meson contributions to the effective interaction in the $pp$ channel $v_{pp}(k,p)$ as a function of $p$ at $k = k_{\rm F} = 0.9$ fm$^{-1}$ with the effective interaction, PK1, are shown in Fig. 4. The sum of all the meson contributions results in considerable repulsive interactions for momenta larger than about 1.5 fm$^{-1}$, which is a remarkably different situation from that modeled by the Gogny force calculation.[19]

### 3.2. *The momentum dependence of the pairing gap*

For a given $v_{pp}(k,p)$, the momentum dependence of the pairing gap $\Delta(k)$ can be obtained from Eq. (16). The momentum dependence of $\Delta(k)$ for different Fermi momenta is shown in Fig. 5. The pairing gap has large and positive values at small momenta, then decreases with the momentum and changes its sign around 2.5 fm$^{-1}$. It continues to decrease till $\sim$4.0 fm$^{-1}$, then slowly goes to zero. The difference in pairing gaps for different Fermi momenta is revealed mainly by the behaviors at low momentum. At zero momentum, the largest pairing gap occurs at a Fermi momentum of 0.9 fm$^{-1}$.

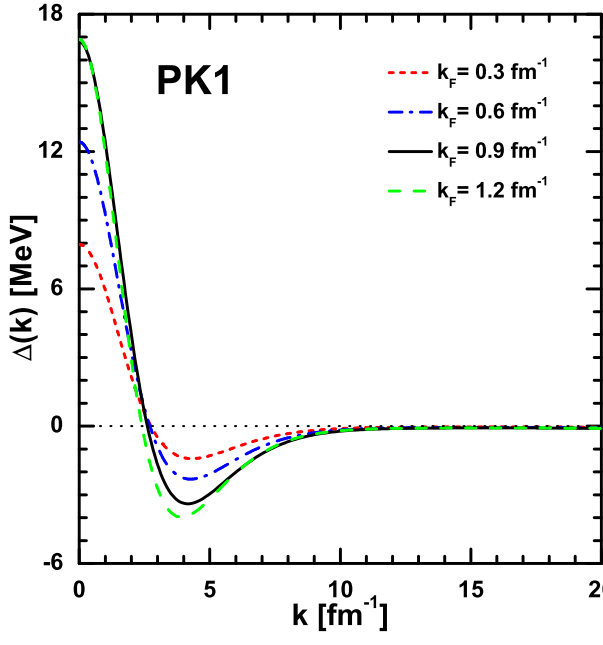


Fig. 5. (Color online) The pairing gap $\Delta(k)$ as a function of the momentum $k$ for Fermi momenta $k_{\rm F} = 0.3$, 0.6, 0.9 and 1.2 fm$^{-1}$ with the effective interaction, PK1.

### 3.3. *The pairing gap at the Fermi surface*

One of most important properties of the pairing gap is its value at the Fermi surface. In Fig. 6, the pairing gap $\Delta(k_{\rm F})$ at the Fermi surface as a function of the Fermi momentum $k_{\rm F}$ with the effective interaction, PK1, is compared to the results obtained with the effective interactions, NL1,[28] NL2,[29] NL3,[30] NLSH,[31] TM1[32] and the results calculated with Gogny force and Bonn potential.[21]

It is found that the pairing gap $\Delta(k_{\rm F})$ is strongly dependent on the nuclear matter density, or equivalently, the Fermi momentum. The pairing gap $\Delta(k_{\rm F})$ increases

with Fermi momentum (or density), reaches a maximum at a Fermi momentum of $k_{\rm F} \approx 0.9$ fm$^{-1}$, and then rapidly drops to zero. Usually, the pairing gap at the Fermi surface calculated with RMF effective interactions is almost three times larger than the value calculated with the Gogny force. Moreover, the pairing gap at lower Fermi momenta does not vanish in calculations with RMF effective interactions, while it does vanish in calculations with the Gogny force or the Bonn potential.

These differences come from the integral in Eq. (16) for the pairing gap, which depends on the products of pairing gap parameter $\Delta(p)$ and the effective interaction in the $pp$ channel $v_{pp}(k,p)$. From $v_{pp}(k,p)$ in Fig. 2 and $\Delta(p)$ in Fig. 5, it is found that considerable contributions to the integral in Eq. (16) may come from the high momenta region. While the various effective forces in RMF models are adjusted for mean-field calculations in the Hartree channel only, i.e. they are only valid for momenta below the Fermi momentum,[19] a realistic interaction in the $pp$ channel $v_{pp}(k,p)$ can exhibit a very different behavior at high momenta.

Considering that RMF effective interactions give a pairing field that is much too strong, an effective factor is introduced in the particle–particle channel to reduce the pairing gap. For PK1, if a factor $f = 0.76$ is introduced, the resulting pairing gap is almost the same as those with the Gogny force or Bonn potential, and a maximum pairing gap 3.2 MeV is obtained at a Fermi momentum of 0.9 fm$^{-1}$, as shown in Fig. 6.

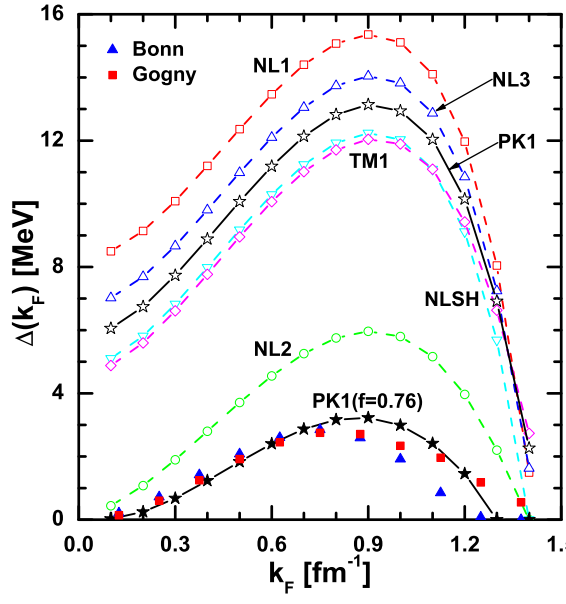


Fig. 6. (Color online) The pairing gap $\Delta(k_{\rm F})$ at the Fermi surface as a function of the Fermi momentum $k_{\rm F}$ for different effective interactions. The results for Gogny and Bonn come from Ref. 21.

## 4. Summary

The pairing properties in the $^1S_0$ channel for symmetric nuclear matter have been studied in the RMF theory with the effective interaction, PK1. The one-meson exchange potential is used in the particle–particle channel consistent with the particle–hole channel. The effective interaction in the *pp* channel is found to be attractive at small momenta with an attractive range around 1.5 $fm^{-1}$ and repulsive at large momenta. The pairing gap at the Fermi surface is strongly dependent on the nuclear matter density, growing as the Fermi momentum increases, reaching its maximum values at a Fermi momentum of around 0.9 $fm^{-1}$, and then dropping to zero rapidly. Considering the fact that the pairing gap at Fermi momenta calculated with RMF effective interactions are three times larger than that with the Gogny force, an effective factor in the particle–particle channel is introduced. For the effective interaction, PK1, a factor $f = 0.76$ will produce almost the same results as those with the Gogny force or with the Bonn potential.

## Acknowledgments

This work is partly supported by the Major State Basic Research Development Program (2007CB815000) and the National Natural Science Foundation of China (10435010, 10775004 and 10221003).

## References

1. J. D. Walecka, *Ann. Phys.* **83** (1974) 491.
2. N. K. Glendenning, *Compact Stars*, 2nd Edn. (Springer-Verlag, New York, 2000).
3. B. D. Serot and J. D. Walecka, *Adv. Nucl. Phys.* **16** (1986) 1.
4. P. G. Reinhard, *Rep. Prog. Phys.* **52** (1989) 439.
5. P. Ring, *Prog. Part. Nucl. Phys.* **37** (1996) 193.
6. J. Meng, H. Toki, S. G. Zhou, S. Q. Zhang, W. H. Long and L. S. Geng, *Prog. Part. Nucl. Phys.* **57** (2006) 470.
7. J. Meng and P. Ring, *Phys. Rev. Lett.* **77** (1996) 3963.
8. J. Meng, *Nucl. Phys. A* **635** (1998) 3.
9. J. Meng and P. Ring, *Phys. Rev. Lett.* **80** (1998) 460.
10. A. Arima, M. Harvery and K. Shimizu, *Phys. Lett. B* **30** (1969) 517.
11. K. T. Hecht and A. Adler, *Nucl. Phys. A* **137** (1969) 129.
12. J. N. Ginocchio, *Phys. Rev. Lett.* **78** (1997) 436.
13. J. Meng, K. Sugawara-Tanabe, S. Yamaji, P. Ring and A. Arima, *Phys. Rev. C* **58** (1998) R628.
14. J. Meng, K. Sugawara-Tanabe, S. Yamaji and A. Arima, *Phys. Rev. C* **59** (1999) 154.
15. T. S. Chen, H. F. Lü, J. Meng, S. Q. Zhang and S. G. Zhou, *Chin. Phys. Lett.* **20** (2003) 358.
16. S.-G. Zhou, J. Meng and P. Ring, *Phys. Rev. Lett.* **91** (2003) 262501.
17. A. Bohr, B. R. Mottelson and D. Pines, *Phys. Rev.* **110** (1958) 936.
18. P. W. Anderson and N. Itoh, *Nature* (*London*) **256** (1975) 25.
19. H. Kucharek and P. Ring, *Z. Phys.* **339** (1991) 23.
20. J. Dechargé and D. Gogny, *Phys. Rev. C* **21** (1980) 1568.
21. M. Serra, A. Rummel and P. Ring, *Phys. Rev. C* **65** (2001) 014304.

22. F. B. Guimaraes, B. V. Carlson and T. Frederico, *Phys. Rev. C* **54** (1996) 2385.
23. M. Matsuzaki, *Phys. Rev. C* **58** (1998) 3407.
24. J. S. Chen, P. F. Zhuang and J. R. Li, *Phys. Lett. B* **585** (2004) 85.
25. M. Matsuzaki and T. Tanigawa, *Phys. Lett. B* **445** (1999) 254.
26. S. Sugimoto, K. Sumiyoshi and H. Toki, *Phys. Rev. C* **64** (2001) 054310.
27. W.-H. Long, J. Meng, V. G. Nguyen and S.-G. Zhou, *Phys. Rev. C* **69** (2004) 034319.
28. P. G. Reinhard *et al.*, *Z. Phys. A* **323** (1986) 13.
29. S.-J. Lee *et al.*, *Phys. Rev. Lett.* **57** (1986) 2916.
30. G. A. Lalazissis, J. Konig and P. Ring, *Phys. Rev. C* **55** (1997) 540.
31. M. M. Sharma, M. A. Nagarajan and P. Ring, *Phys. Lett. B* **312** (1993) 377.
32. Y. Sugahara, H. Toki and P. Ring, *Theor. Phys.* **92** (1994) 803.